BioCore Exploring Scientific Community

International Journal of Nanotechnology in Medicine & Engineering

Research Article ISSN 2474-8811

The size and Surface Effect on Mechanical Behavior of Pd Cubic Nanocrystals under Uniaxial Compression

Lijun Meng*, Haiyan Peng, Yanru Li

Hunan Key Laboratory for Micro-Nano Energy Materials and Devices, Hunan, People's Republic of China
Faculty of Materials and Optoelectronic Physics, Xiangtan University, Xiangtan 411105, Hunan, People's Republic of China

Abstract

We investigated the size and surface effects on mechanical properties of face-centered cubic (FCC) Pd nanocrystals (NC) in cubic shape under uniaxial compression using atomistic simulation techniques. The results revealed that mechanical behavior of Pd nanocrystals is highly dependent on the size and surface structure. The critical stress (strain) for Pd nanocrystals with {100} lateral surfaces decrease monotonically as the increasing size, which is consistent with the well-known Hall-Petch relation. In contrast, the critical stress (strain) for nanocrystals with {110} lateral surfaces manifests an inverse Hall-Petch relation. We also demonstrated different initial dislocation structures in incipient stage of plastic deformation by analyzing von Mises stress and slip vector. Interestingly, the dislocation sources strongly depend on atom arrangements at contact surfaces. This contact-surface-control mechanical response model can be applied to study mechanical properties of other noble metal nanocrystals.

Keywords: Nanocrystals; Molecular dynamics; Nanocompression; Mechanical behavior

Corresponding author: **Lijun Meng**

Hunan Key Laboratory for Micro-Nano Energy Materials andDevices, Hunan, People's Republic of China Tel : 07712808567

Email: mljphy@qq.com

Citation: Lijun Meng et al. (2019) The size and Surface Effect on Mechanical Behavior of Pd Cubic Nanocrystals under Uniaxial Compression. Int J Nano Med & Eng. 4:3, 26-32

Received: June 11, 2019
Accepted: June 21, 2019
Published: July 20, 2019

Introduction

Nanosize materials have attracted considerable interest for improving our understanding of material plasticity and providing design guidelines for nano- electromechanical devices [1-7]. Due to the smaller size and larger surface/volume ratio these materials often possess unusual mechanical properties that be markedly differ from those of their bulk counterparts [8-14]. Recently, a new nanocompression technique to explore mechanical properties of nanomaterials was developed [3, 6, 14, 16]. The newly developed technique using a diamond-anvil cell (DAC) has been used to explore the mechanical behaviors of nanocrystals and improve our understanding of mechanical properties of nanosized particles. For example, Q.X. Guo et al. observed a phase transformation from FCC to face-centered tetragonal (FCT) in the cold-compressed Pd nanocubes [3]. Previous studies on high pressure behaviors of NCs also identify the size-dependence of critical stress, critical strain, dislocation structures, and so on. The surface and structural features affecting mechanical properties were discussed in the literatures, but the mechanisms of deformation have not been completely understood at atomic level. Nanocompression, in combining with real-space techniques such as atomic force microscopy (AFM) or transmission electron microscopy (TEM), provides an important tool to explore the relationship of mechanical properties and surface structures. But it is difficult to obtain the atomic-level information during the microcompression process and to observe the motion of an individual dislocation. The molecular simulation as a powerful tool has been widely used to study the mechanical response of semiconductor and metal nanocrystals such as SiC [4], Si [9, 17, 18], Au [16], Al [19]. For example, J. Munilla et al., focusing mainly on the effects of the small scale and the surface, have investigated the mechanical properties of Al nanocrystals [19]. Most of studies using molecular simulation method have focused mainly on nanopillars and polycrystalline materials, while little efforts have been devoted to mechanical properties of nanosize single-crystal materials [16, 21]. Dan Mordehai et al. [16] have studied size effect and dislocation nucleation in compression of single-crystal gold microparticles.

The size and surface effect become dominant factors to influence mechanical behavior of nanocrystals. Previous studies have shown the Hall-Petch size-dependence of yielding strength in the micro-tensile/compression experiments of nanocrystals. The inverse Hall-Petch relation has also been evidenced in some nanosize systems such as PdTe nanocrystals [11]. Many models have been proposed to explain the size-dependence of the yielding stress such as dislocation-starvation model and surface-controlled dislocation multiplication model [20]. The surface due to asymmetric release of stress becomes dislocation source which leads to complex dislocation structure in the large surface/volume ratio nanocrystals. In present work, we investigated

the compression behaviors of FCC Pd nanocrystals using molecular simulation techniques. By modeling nanocrystals with different sizes and different lateral surfaces, we have carried out a series of compression simulations in order to explore the effect of these factors on the mechanical properties of FCC Pd nanocrystals.

The method of calculations

The noble metal Pd nanocrystals have attracted much attention for applications in efficient catalysis. The synthesized Pd nanocrystals using chemical vapor deposition (CVD) have faceted structures such as nanocubes [3,22]. The nanocubic structure oriented in the [001] direction are terminated generally by {100} or {110} lateral surfaces.

Fig. 1(a) shows a schematic illustration of nanocompression and contact surfaces between nanocrystal and indenters. The cubic-shaped nanocrystals with edge length in the size range of 1-20nm (~1.0×102-5.0×105 atoms) were prepared by cutting a perfect FCC of Pd with a lattice constant of 3.89 Å. In order to explore surface effects, we have modeled the {110} and {100} lateral surface cubic nanocrystals (denoted as {110}-NC and {100}-NC, respectively) which both oriented in the [001] direction. Two planar nanoindenters have been positioned respectively on the top and bottom of NC and move toward the surfaces of NC along [001] and [00-1] direction. Notice that the contact surfaces between top/bottom surfaces and indenters exists two (three) possible atom arrangements for {110}-NC ({100}-NC). There are two type contact surfaces in {110}-NC as shown in Fig.1 (b). The area of surface is larger than that of subsurface which results in edge atoms in the contact surface (case 1, left panel in fig.1(b)). On the contrary, the smaller surface area leads to the lack edge atoms in the contact surface (case 2, right panel in fig.1(b)). As a consequence, we can classify nanocrystals into three categories: {110}-NC1 ({110}-NC2) without (with) edge atoms at both contact surfaces and {110}-NC3 with edge atoms at arbitrary contact surfaces. These {110} lateral surface NCs demonstrate markedly different nucleation mechanism of dislocations and stress-strain behaviors. Similarly, we can classify three types of contact surfaces in the {100}-NC according to the distribution of vertex atoms in nanocube as depicted in Fig.1(c). The mechanical response of NC displays the significant difference due to different arrangement at contact surfaces. Our simulation results identify that atom distribution at contact surfaces has relatively little influence on critical strain and stress but crucial effect on the nucleation and propagation of dislocations for {100}-NC.

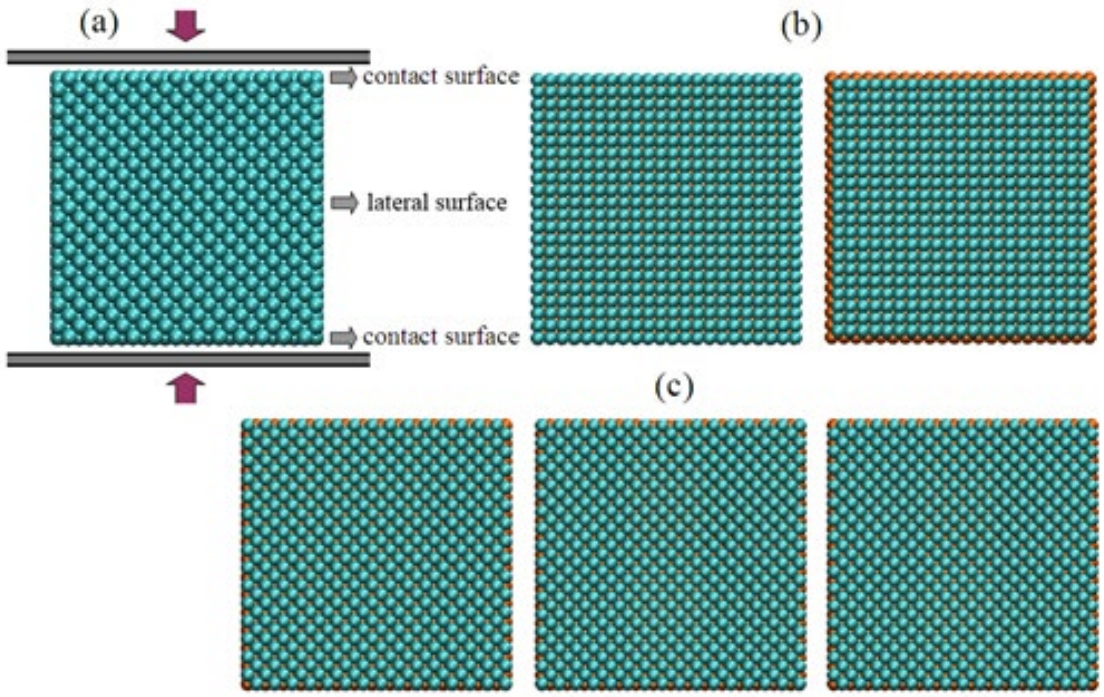

Fig. 1 (a) Nanocompression model. Top and bottom gray planes denote indenters and purple arrows represent the direction of compression. Cubic-shaped Pd nanocrystal was positioned between two indenters with cyan balls standing for Pd atoms. (b) Two possible contact surfaces nanocrystals with {110} lateral surfaces ({110}-NC). Left (case 1): the contact surface area is larger than that of subsurface. Right (case 2): the surface area is smaller than that of subsurface. Different atom distributions in both cases influence importantly on not only critical stress (strain) but also initial dislocation structures under uniaxial compression. (c) Three possible contact surfaces nanocrystals with {100} lateral surfaces ({100}-NC) according to vertex atoms distribution. It is notice that there are two (left), four (middle) or zero (right) atoms at the corner of contact surface. The cyan (orange) balls represent surface (subsurface) atoms.

We carried out extensively molecular dynamics simulations under uniaxial compression along [001] direction for all cubic nanocrystals. The nanocompression simulations were performed using a parallel MD code, LAMMPS, developed by Plimpton and co-workers [23]. The interatomic interaction of Pd atoms is described by an embedded atom method (EAM) potential that used widely for metal elements and their alloys [23-25]. The repulsive force between nanocrystal and indenter was added directly in LAMMPS code. Our simulations include two basic steps. First, the indenters keep static and nanocrystals have been relaxed up to 2ps at lower temperature 0.001K in order to eliminate thermal effect. In the second step, the rigid top (bottom) indenter moves toward down (up) with constant speed, leading to a uniaxial compression of nanocrystals. We defined zero strain as zero-loading exerting on the nanocrystals and obtained the critical strain (stress) that corresponds to an abrupt drop in the strain-stress curve. In our simulations, we control the strain rate by adjusting the movement speed of indenters.

We firstly performed compression simulations under different strain rate ranging from about 107/s to 108/s in order to study the influence of strain rate on the deformation process. The strain-stress curve for a typical nanocrystal with {110} lateral surface and edge length 11.51nm has shown in Fig. 2. The compression deformation process includes generally three typical stages: elastic, homogenously plastic, heterogeneously deformation. Stress increases almost linearly with strain in the incipient stage of elastic process and then increases nonlinearly due to the ductile of metal material and the formation of surface defects [19]. In our simulations, the stress-strain curves in these stages have a similar characteristic. Subsequently, the stress reaches maximal value corresponding to the critical stress (yielding point) and then drops abruptly. Then the system enters into the plastic deformation stage and some nucleation sites of dislocation start to appear. The dislocation nucleates and propagates gradually as the increase of strain and results in the irregular fluctuation of stress.

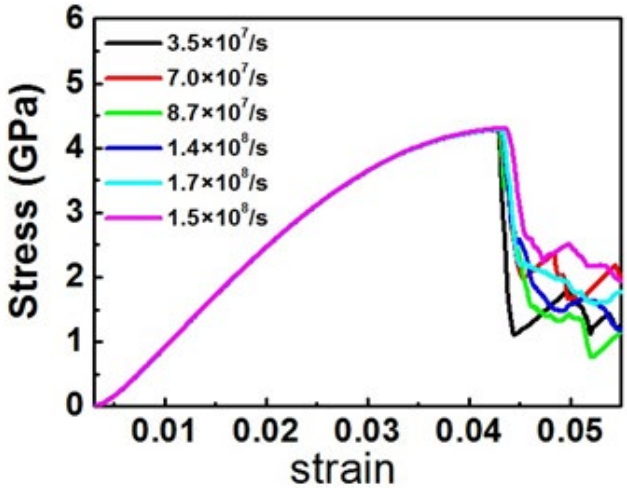

Fig 2: The stress-strain curve at the different strain rate for Pd nanocrystal with edge length 11.51nm.

Results and discussion

The strain-stress curves for both {100}-NCs and {110}-NCs with different size ranging from 1~20nm have shown in Fig. 3. The critical yield strength and yield strain vary with the size and surface structures of nanocrystals. The variation of critical strain and stress as a function of size has shown in Fig. 4. For {100}-NC, the critical stress (strain) decrease monotonically with the increasing edge length besides little fluctuation. The little fluctuation reflects different dislocation nucleation and will discuss in details later. The critical stress (strain) decreases slowly and tends to reach a stable value about 4.2GPa (0.40) within the size range of our simulations. The resulting size dependence is consistent with the Hall-Petch relation found in other FCC nanomaterials [16].

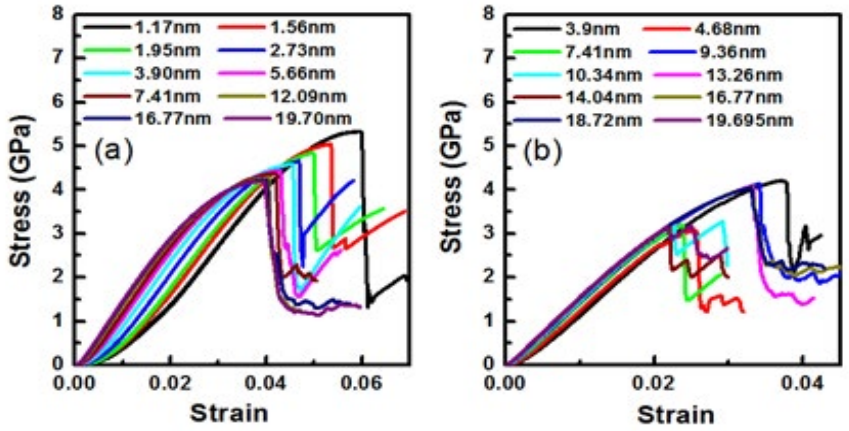

Fig. 3: The strain-stress curves of nanocrystals with different size and lateral surfaces: (a) the {100}-NCs; (b) the {110}-NCs.

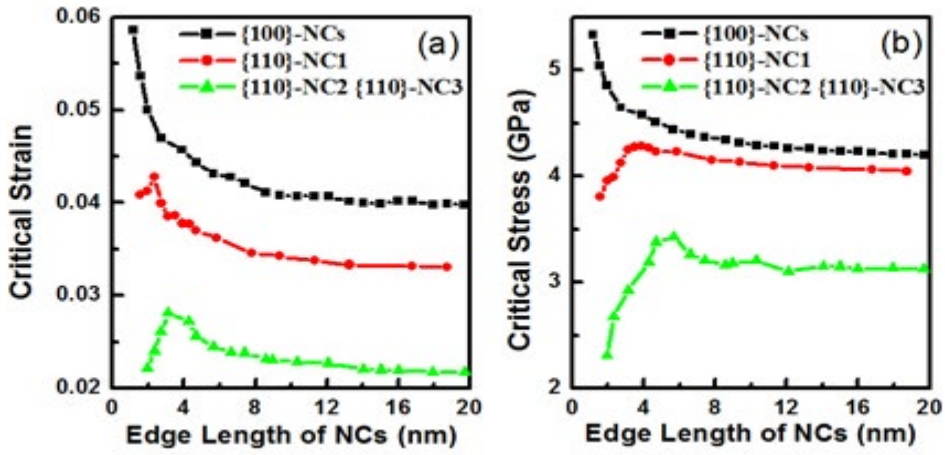

Fig. 4: The size dependence of critical strain (a) and critical stress (b). The critical stress (strain) shows a Hall-Petch relation for {100}-NCs and an inverse Hall-Petch relation for {110}-NCs. The {110}-NC1 ({110}-NC2, {110}-NC3) represents {110} lateral surface NCs without (with) edge atoms at contact surfaces.

As shown in Fig.4, the critical stresses of {110}-NCs are smaller than those of {100}-NCs and exhibit a non-monotonically size dependence. In contrast to {100}-NCs, the critical stress (strain) increase initially and then decrease as increasing size, which give a maximum critical stress (strain) in size about 4nm. This inverse Hall-Petch relation was also studied in other semiconductor nanocrystals and crystalline materials [11, 12]. Moreover, the critical stress (strain) demonstrates markedly different behavior due to atom arrangements at the contact surfaces. The critical stresses (strains) of nanocrystals with edge-vertex atoms ({110}-NC2, {110}-NC3) are obviously smaller than those of nanocrystals without edge-vertex atoms at both contact surfaces ({110}-NC1).

In order to address the distinct mechanical behaviors of both {100}-NCs and {110}-NCs, we calculated the distribution of von Mises stress. The von Mises stress can be calculated using Cauchy stress tensor [26], which shown in Fig. 5 and Fig. 6. Moreover, we have studied dislocation nucleation and propagation by slip vector analysis (SVA) technique. The slip vector, a quantity closely related to the Burgers vector, has become an important tool to analyze mechanical properties of nanomaterials [15, 17, 27]. The SVA can describe quantitatively the dislocation nucleation and propagation during the compression deformation and is defined as

$$s_i = -\frac{1}{N_s}\sum_{j=i}^{N_{nn}}(r_{ij} - r_{ij}^0),$$

,

where rij and rijo are the vectors linking atom i and all its Nnn nearest neighbors j in the current and reference positions, respectively. Ns stands for the number of slipped neighbors. The spatial distributions of slip vector moduli |si| with a suitable color scale are shown in Fig.5 and Fig.6.

For {100}-NCs, there are three possible contact surfaces that rely on vertex atoms distribution as illustrated in Fig.1 (c). The vertex atoms affect greatly the nucleation of dislocation, but only little effect on critical stress. Under external pressure, due to the little constrain

compares to interior atoms, these vertex atoms release stress and lead to local lattice deformation in the corner of cubic nanocrystals. The von Mises stresses of edge atoms of subsurface accumulate rapidly as the increasing strain due to local lattice deformation. In contrast, the stress release for the NCs without vertex atoms can be accomplished by propagating into the edge-atoms of subsurface. The von Mises stresses of these atoms reach firstly a critical yielding stress and lead to nucleation sites of dislocation. Under increasing pressure, these dislocations glide rapidly away from their sources within the {111} crystal planes due to smaller resistance, and escape the particle through surfaces, leaving behind surface steps [16]. In incipient stage of plastic deformation, four slip planes propagate rapidly in the interior of nanocrystal and form tetrahedron-like dislocation structure as shown in Fig.5 b.

We noted that, for the NCs without vertex atoms in eight corners, the edge-atoms of lateral surfaces also form the nucleation site but need a larger pressure, and result in eight slip planes finally. These slip planes penetrate each other and terminate finally at the surface. As the increase of strain, more nucleate sites and slip planes emerge. These increasing slip planes meet finally each other and form complex labyrinth-like slip system. As a result, there are two dislocation structures in the early stage of plastic deformation due to three vertex atoms distributions as shown in down panel of Fig.5.(a). The critical stresses of nucleation are nearly same on both cases and almost independent of the size of NCs. The size dependence of critical stress (strain) can be attributed to the stress gradient in slip planes [16], which in turn, depends on the specimen size and consistent with the Hall-Petch relation.

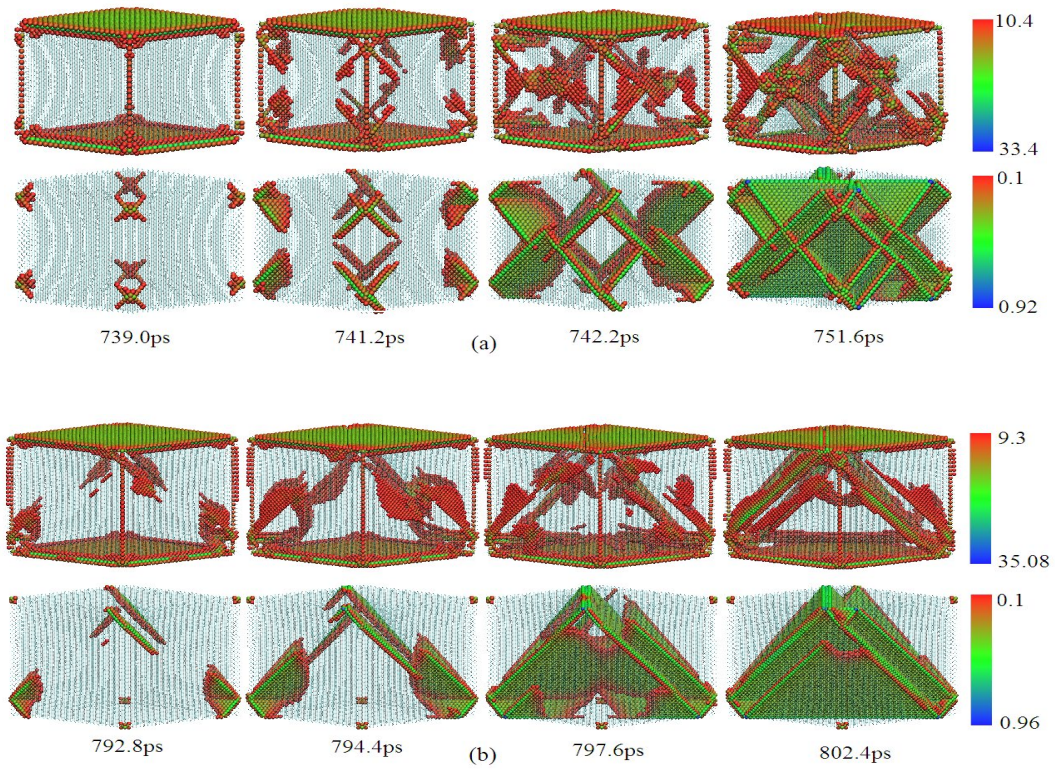

Fig. 5: The von Mises stress and slip vector representation of dislocation at different strain for {100}-NC. (a) The nanocrystal with edge length 8.58nm (45562 atoms): the nucleation of dislocation appears first for the side-edge atoms and slip rapidly on {111} crystal planes, then form eight slip planes and finally resulting in labyrinth-like dislocation structure. Upper panel shows the von Mises stress and lower panel show the slip vector representation of dislocation. (b) The nanocrystal with edge length 11.51nm (108000 atoms). Four slip planes form a pyramid-like dislocation structures. Only defective atoms are displayed according to their von Mises stress (see bar scale). The cyan points stand for Pd atoms that color value are under the corresponding color scale.

For {110}-NC, edge atoms of contact surfaces influence importantly on not only the nucleation of dislocation but also the critical yielding stress and strain. As we pointed in previous section, the {110}-NCs can be classified into three types: {110}-NC1, {110}-NC2 and {110}-NC3. From our simulations, two initial dislocation structures corresponding to NC1/NC2 and NC3 have been identified using slip vector analysis. This discrepancy between NC1/NC2 and NC3 can be explained by different accumulation model of stress. The von Mises stress and slip vector for a typical nanocrystal with edge length 10.335nm are shown in Fig. 6. An asymmetric distribution of the von Mises stress at both contact surfaces can be found for NC1/NC2. During compression process, the von Mises stress of edge-vertex atoms at subsurface increases and firstly reaches the critical stress due to its fast accumulation at the case I surface (with vertex atoms at contact surface). These stress concentrated atoms form firstly nucleation sites of dislocation as approaching to yielding point. Subsequently, these initial dislocations extend quickly along edges of contact surfaces and glide rapidly on {111} crystal planes under relatively smaller external pressure. Four slip planes form finally a pyramid-like slip system in the interior of nanocrystal as shown in down panel of Fig. 6 (b).

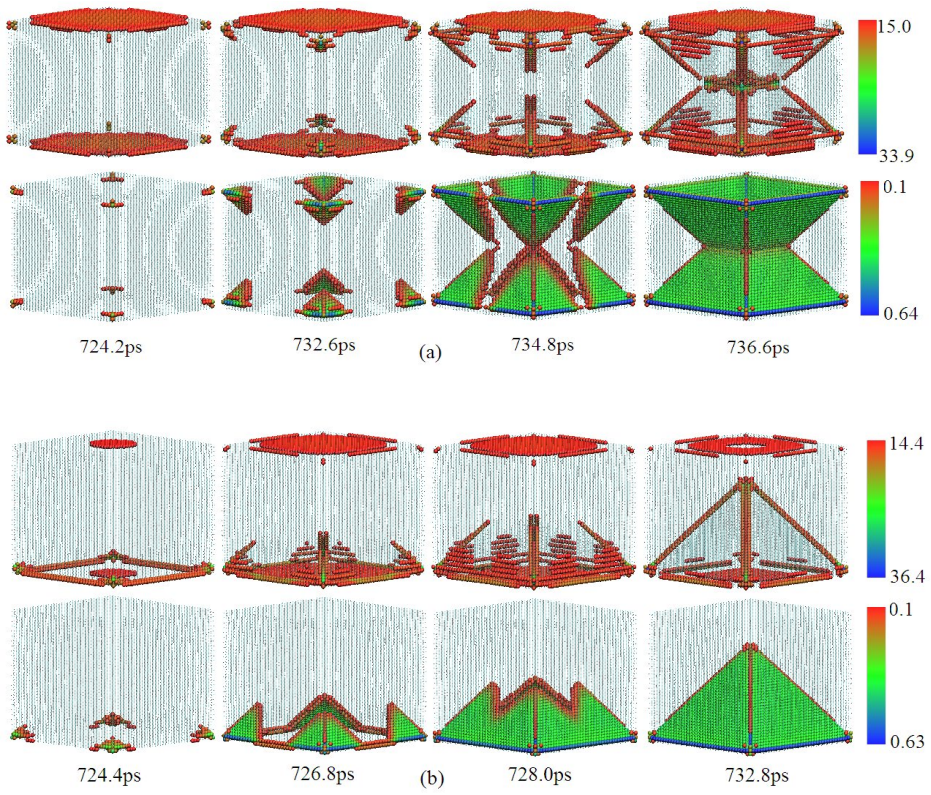

Fig. 6: The von Mises stress distribution and slip vector representation of dislocation at different strain for {110}-NCs. (a) The {110}-NC1 with edge length 9.36nm (58300 atoms) and (b) The {110}-NC3 with edge length 10.34nm (80055 atoms). In both cases, the nucleation of dislocation takes place at the lateral-edge atoms that glide on {111} crystal planes, and finally forms sandglass- and pyramid-like dislocation structures respectively. Note that the increase of stress at bottom contact surface is faster than that of the top contact surface and leading to nucleation asymmetrically for {110}-NC3.

However, for case II surface (without vertex atoms at contact surface), it is relatively difficult to nucleate at the subsurface, which result in larger yield strength. Therefore, the nanocrystals that possess edges atoms at top/bottom surfaces have the smallest yield strength, but nanocrystals without edges atoms have the largest yield strength. The resulting dislocation in both cases encounter each other in the core of NCs and form sandglass-like dislocation structure in the early stage of plastic deformation. The new dislocation sources emerge at the core region as further increase of strain. For the smaller nanocrystals (edge length < ~3.8nm), more dislocation sources are produced not only at side-edges but also at the edges of contact surfaces, which lead to more complex dislocation structures. Consequently, the yielding strength for NCs with size ranging from 1 to 3.8 nm increases with the increasing size, which in turn, results in the reverse Hall-Petch relation.

Conclusions

In summary, we investigated the size and surface effects on mechanical properties of FCC metal Pd cubic nanocrystals using molecular simulation techniques. The results demonstrated markedly different mechanical behaviors of size- and surface-dependence on critical strain and stress. The critical stress (strain) for {100}-NCs decreases monotonically with the increasing size, which is agreement with the Hall-Petch relation. In contrast, the critical stress (strain) for {110}-NCs exhibits a non-monotonically dependence on size and contact surfaces. The critical stress (strain) increases first and then decreases as the increasing size. We have analyzed dislocation nucleation through von Mises stress and found that the corners of NCs control greatly dislocation nucleation. Using slip vector analysis technique, we have found different initial dislocation structures for both types of nanocrystals. For {100}-NCs, four or eight slip planes formed in the incipient stage of plastic deformation encounter and lead to labyrinth- and tetrahedron-like dislocation structures. In contrast, for {110}-NCs, four or eight slip planes propagate on the {111} crystal planes and result in sandglass- and pyramid-like dislocation systems. Our simulation results identified that dislocation sources are originated from the surface edges of nanocrystals, which is consistent with a surface-control nucleation model. However, the atom arrangements of contact surfaces influence significantly mechanical properties of nanocrystals. The initial dislocation structure and dislocation formation mechanisms provide possible insights into the pressure-induced behaviors of other noble metal FCC nanocrystals.

Acknowledgements

This work is supported by the National Natural Science Foundation of China (Grant No. 11204261) and National Natural Science Foundation of Hunan Province(Grant No . 2018JJ2381)

References

[1] K. Zheng, C. C. Wang, Y. Q. Cheng, Y. H. Yue, X. D. Han, Z. Zhang, Z. W. Shan, S. X. Mao, M. M. Ye, Y. D. Yin, E. Ma, Electron-beam-assisted superplastic shaping of nanoscale amorphous silica, Nat. Commun. 10 (2010) 1028.

[2] F. Ge, W.F. Li, X. M. Shen, J. M. Perez-Aguilar, Y. Chong, X.F. Gao, Z.F. Chai, C.Y. Chen, C.C. Ge and R.H. Zhou, Differential Pd-nanocrystal facets demonstrate distinct antibacterial activity against Gram-positive and Gram-negative bacteria, Nat. Commun. 9, (2018),129

[3] Q. X. Guo, Y. S. Zhao, W. L. Mao, Z. W. Wang, Y. J. Xiong, Y N Xia, Cubic to tetragonal phase transformation in cold-compressed Pd nanocubes, Nano Lett. 8 (2008) 972-975.

[4] Q. X. He, J. Fei, C. Tang, J. X. Zhong, L. J. Meng, Mechanical behavior of silicon carbide nanoparticles under uniaxial compression, J. Nanopart. Res. 18 (2016) 68.

[5] S. W. Lee, L. Meza, J. R. Greer, Cryogenic nanoindentation size effect in [0 0 1]-oriented face-centered cubic and body-centered cubic single crystals, Appl. Phys. Lett. 103 (2013) 101906.

[6] P. Valentini, W. W. Gerberich, T. Dumitrica, Phase-transition plasticity response in uniaxially compressed silicon nanospheres, Phys. Rev. Lett. 99 (2007) 175701.

[7] A. S. Mikheykin, V. P. Dmitriev, S. V. Chagovets, A. B. Kuriganova, N. V. Smirnova, I. N. Leontyev, The compressibility of nanocrystalline Pt, App. Phys. Lett. 101 (2012) 173111.

[8] Jonathan Amodeo,Khalid Lizoul, Mechanical properties and dislocation nucleation in nanocrystals with blunt edges, Materials & Design,135, (2017) 223-231

[9] Eric N.HahnabSaryu J.FensinaTimothy C.Germannb George T.GrayIII,Orientation dependent spall strength of tantalum single crystals, Acta Materialia,159 15 (2018) 241-248

[10] KaiXiong, HaimingLu, JianfengGu, Atomistic simulations of the nanoindentation-induced incipient plasticity in Ni3Al crystal, Computational Materials Science, 1151(2016) 214-226

[11] Z. W. Quan, Y. X. Wang, I. T. Bae, W. S. Loc, C. Y. Wang, Z. W. Wang, J. Y. Fang, Reversal of Hall–Petch Effect in Structural stability of PbTe nanocrystals and associated variation of phase transformation, Nano Lett. 11 (2011) 5531 -5536.

[12] J. B. Jeon, B. J. Lee, Y. W. Chang, Molecular dynamics simulation study of the effect of grain size on the deformation behavior of nanocrystalline body-centered cubic iron, Scripta Mater. 64 (2011) 494-497.

[13] D.Kilymisa,C.Gérarda,J.Amodeob,U.V.Waghmarec,L.Pizzagalli, Uniaxial compression of silicon nanoparticles: An atomistic study on the shape and size effects, Acta Materialia 158 1 (2018) 155-166

[14] V. Swamy, A. Y. Kuznetsov, L. S. Dubrovinsky, A. Kurnosov, V. B. Prakapenka, Unusual compression behavior of anatase TiO2 nanocrystals, Phys. Rev. Lett. 103 (2009) 075505

[15] O. R. de la Fuente, J. A. Zimmerman, M. A. Gonzalez, J. de la Figuera, J. C. Hamilton, W. W. Pai, J. M. Rojo, Dislocation emission around nanoindentations on a (001) fcc metal surface studied by scanning tunneling microscopy and atomistic simulations, Phys. Rev. Lett. 88 (2002) 036101.

[16] D. Mordehai, S. W. Lee, B. Backes, D. J. Srolovitz, W. D. Nix, E. Rabkin, Size effect in compression of single-crystal gold microparticles, Acta Mater. 59 (2011) 5202-5215.

[17] N. Zhang, Q. Deng, Y. Hong, L. M. Xiong, S. Li, M. Strasberg, Deformation mechanisms in silicon nanoparticles, J. App. Phys. 109 (2011) 063634.

[18] L.Yang, J. J. Bian, H. Zhang, X. R. Niu,G. F. Wang, Size-dependent deformation mechanisms in hollow silicon nanoparticles, AIP Advances 5(2015) 077162.

[19] J. Munilla, M. Castro, A. Carnicero, Surface effects in atomistic mechanical simulations of Al nanocrystals, Phys. Rev. B 80 (2009) 024109.

[20] C. R. Weinberger W. Cai, Surface-controlled dislocation multiplication in metal micropillars, Proc. Natl. Acad. Sci. 105 (2008) 14304-14307.

[21] R. Kositski, D. Mordehai, Depinning-controlled plastic deformation during nanoindentation of BCC iron thin films and nanoparticles, Acta Mater. 15 (2015) 370–379.

[22] X. Q. Huang, Y. J. Li, Y. J. Li, H. L. Zhou, X. F. Duan, Y. Huang, Synthesis of PtPd bimetal nanocrystals with controllable shape, composition, and their tunable catalytic properties, Nano Lett. 12 (2012) 4265-4270.

[23] S. Plimpton, Fast Parallel Algorithms for short-range molecular dynamics, J. Comp. Phys. 117 (1995) 1-19.

[24] X. W. Zhou, R. A. Johnson, H. N. G. Wadley, Misfit-energy-increasing dislocations in vapor-deposited CoFe/NiFe multilayers, Phys. Rev. B 69 (2004) 144113.

[25] L. J. Meng, X. Y. Peng, K. W. Zhang, C. Tang, J. X. Zhong, Structural phase transitions of FeCo and FeNi nanoparticles: A molecular dynamics study, J. Appl. Phys. 111 (2012) 024303.

[26] B. Arman, S. N. Luo, T. C. Germann, T. Cagin, Dynamic response of Cu46Zr54 metallic glass to high-strain-rate shock loading: Plasticity, spall, and atomic-level structures, Phys. Rev. B 81 (2010) 144201.

[27] J. A. Zimmerman, C. L. Kelchner, P. A. Klein, J. C. Hamilton, S. M. Foiles, Surface step effects on nanoindentation, Phys. Rev. Lett. 87 (2001) 165507.